Steroid receptor coactivator-2 (SRC-2) coordinates cardiomyocyte paracrine signaling to promote pressure overload–induced angiogenesis

Received for publication, June 29, 2017, and in revised form, November 9, 2017 Published, Papers in Press, November 10, 2017, DOI 10.1074/jbc.M117.804740

Ji Ho Suh[‡], Li Lai[§], Deokhwa Nam[‡], Jong Kim[¶], Juyeon Jo[‖], George E. Taffet[**], Eunah Kim[‡], Jason T. Kaelber[‡‡], Hyun-Kyoung Lee[‖], Mark L. Entman[**], John P. Cooke[§], and Erin L. Reineke[‡1]

*From the [‡]Center for Bioenergetics and [§]Department of Cardiovascular Sciences, Houston Methodist Research Institute, Houston, Texas 77030, the [¶]University of Houston 77004, Houston, Texas, the [‖]Department of Pediatrics and Neuroscience, Baylor College of Medicine and Neurological Research Institute at Texas Children's Hospital, Houston, Texas 77030, and the **Division of Cardiovascular Sciences, Department of Medicine, and the [‡‡]National Center for Macromolecular Imaging and Department of Molecular Virology and Microbiology, Baylor College of Medicine, Houston, Texas 77030*

Edited by Joel Gottesfeld

Pressure overload–induced cardiac stress induces left ventricular hypertrophy driven by increased cardiomyocyte mass. The increased energetic demand and cardiomyocyte size during hypertrophy necessitate increased fuel and oxygen delivery and stimulate angiogenesis in the left ventricular wall. We have previously shown that the transcriptional regulator steroid receptor coactivator-2 (SRC-2) controls activation of several key cardiac transcription factors and that SRC-2 loss results in extensive cardiac transcriptional remodeling. Pressure overload in mice lacking SRC-2 induces an abrogated hypertrophic response and decreases sustained cardiac function, but the cardiomyocyte-specific effects of SRC-2 in these changes are unknown. Here, we report that cardiomyocyte-specific loss of SRC-2 (SRC-2 CKO) results in a blunted hypertrophy accompanied by a rapid, progressive decrease in cardiac function. We found that SRC-2 CKO mice exhibit markedly decreased left ventricular vasculature in response to transverse aortic constriction, corresponding to decreased expression of the angiogenic factor VEGF. Of note, SRC-2 knockdown in cardiomyocytes decreased VEGF expression and secretion to levels sufficient to blunt *in vitro* tube formation and proliferation of endothelial cells. During pressure overload, both hypertrophic and hypoxic signals can stimulate angiogenesis, both of which stimulated SRC-2 expression *in vitro*. Furthermore, SRC-2 coactivated the transcription factors GATA-binding protein 4 (GATA-4) and hypoxia-inducible factor (HIF)-1α and -2α in response to angiotensin II and hypoxia, respectively, which drive VEGF expression. These results suggest that SRC-2 coordinates cardiomyocyte secretion of VEGF downstream of the two major angiogenic stimuli occurring during pressure overload bridging both hypertrophic and hypoxia-stimulated paracrine signaling.

Cardiac stress induced by pressure overload is characterized by an initial change in metabolic signaling that gives rise to left ventricular hypertrophy driven by increased cardiomyocyte mass. The growing cardiomyocytes send paracrine signals to induce angiogenesis, thus keeping the vasculature in proportion with the ventricle wall mass (1, 2). This hypertrophy-induced signaling is at least partially driven through activation of transcription factor GATA-4, which controls many genes involved with the cardiomyocyte growth, as well as VEGF production and secretion from the cardiomyocyte (3). If angiogenesis is impaired or an imbalance occurs such that wall growth or oxygen demand due to increased workload accelerates faster than new vasculature, local regions of hypoxia arise, leading to activation of hypoxia-inducible factor (HIF)[2]-1α and -2α. Acting through a different cis-element in the VEGF promoter, transcription factors HIF-1α and HIF-2α can further stimulate VEGF expression and secretion from the cardiomyocyte to stimulate angiogenesis (1). Impairment of these responses or sustained load eventually leads to cardiac dysfunction. In a mouse model of pressure overload induced by transverse aortic constriction (TAC), VEGF deficiency resulted in myocardial capillary rarefaction associated with the hypertrophic response, leading to rapid functional decline (4). Conversely, adenoviral delivery of pro-angiogenic factors, including VEGF and angiopoietin-1, can preserve cardiac function during TAC (5–7).

Steroid receptor coactivator-2 (SRC-2) is a transcriptional coactivator that acts as a scaffold for transcription factors to amplify their action, depending on the cellular context and upstream signals. In the heart, we have previously shown that SRC-2 can control the expression and activation of several key cardiac transcription factors, including GATA-4, myocyte

This work was supported by National Institutes of Health Grant R00-HL118159 (to E. L. R.), R01-HL089792 (to M. L. E.), and the Souki Mitochondrial Project Fund. The authors declare that they have no conflicts of interest with the contents of this article. The content is solely the responsibility of the authors and does not necessarily represent the official views of the National Institutes of Health.

This article contains Figs. S1–S3.

[1] To whom correspondence should be addressed: Center for Bioenergetics, Houston Methodist Research Institute, 6670 Bertner Ave., R11-213, Houston, TX 77030. Tel.: 713-363-9933; E-mail: elreineke@houstonmethodist.org.

[2] The abbreviations used are: HIF, hypoxia-inducible factor; TAC, transverse aortic constriction; CKO, cardiomyocyte-specific knockout; HUVEC, human umbilical vein endothelial cell; AngII, angiotensin II; PPAR, peroxisome proliferator–activated receptor; RIPA, radioimmune precipitation assay; qPCR, quantitative PCR.

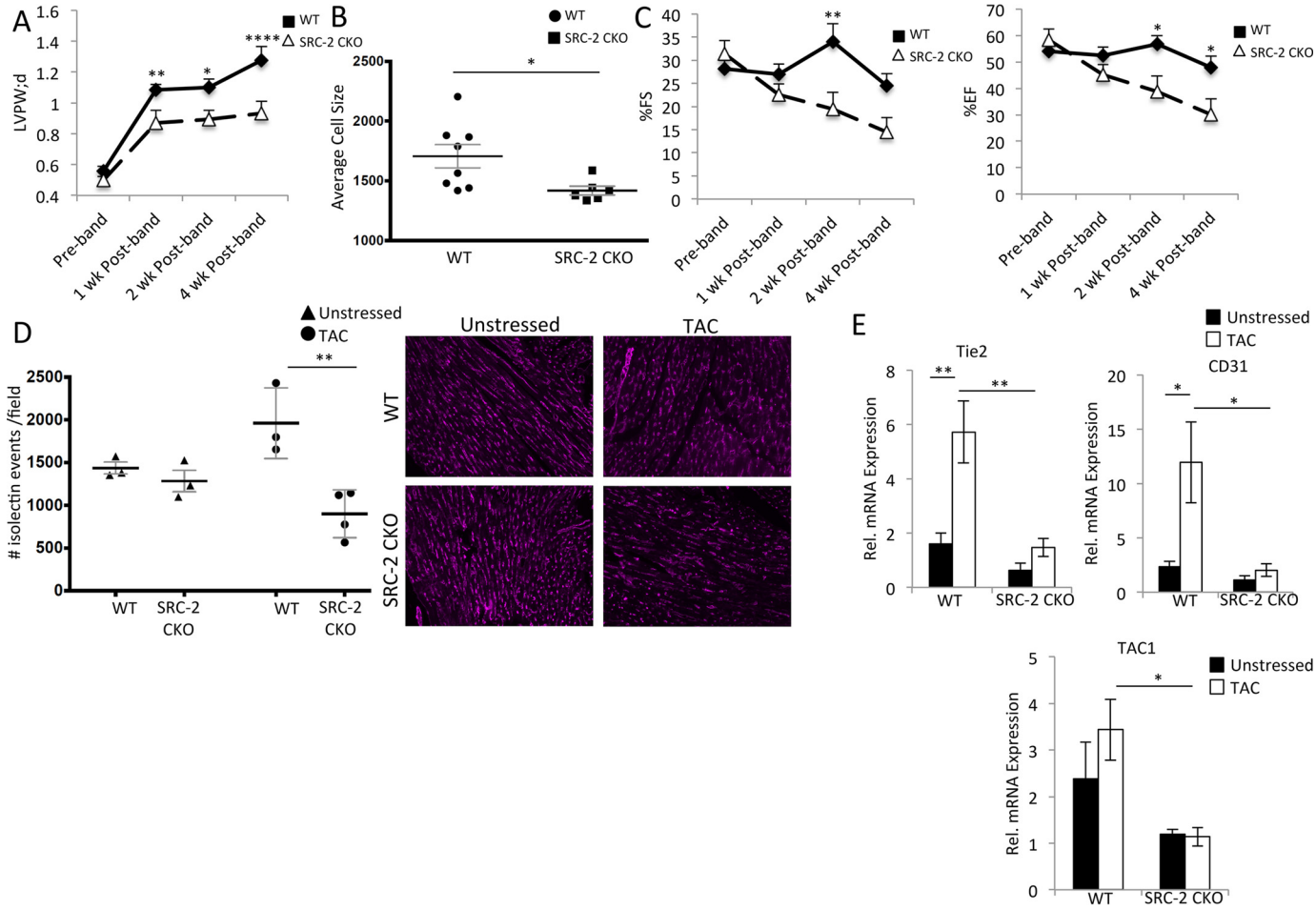

Figure 1. SRC-2 mice have decreased vasculature post-TAC. *A*, left ventricular posterior wall thickness (*LVPW*) echocardiography measurements for WT and SRC-2 CKO mice 4 weeks post-TAC. $n = 7–15$. *B*, heart sections from WT and SRC-2 CKO mice were stained with wheat germ agglutinin (*WGA*), and a cross-sectional area of cardiomyocytes was measured. $n = 8–12$, ≥400 cells/mouse. *C*, percentage ejection fraction and fractional shortening derived from echocardiography as described in *A*. *D*, isolectin staining of heart sections as in *B*. Number of vessels per microscope field is graphed. $n = 3$ mice with 4 sections/mouse analyzed. *E*, qPCR was performed for the indicated genes on total heart RNA from WT and SRC-2 CKO hearts before and 4 weeks after TAC. Rpl32 is used as an internal control, and data are presented relative to unstressed WT. $n = 4$. *, $p \leq 0.05$; **, $p \leq 0.01$; ****, $p \leq 0.0001$. *Tie2*, tyrosine kinase with immunoglobulin-like and EGF-like domains 2; *TAC1*, tachykinin precursor-1. *Error bars*, S.E.

enhancer factor (MEF2), and T-box transcription factor 5 (Tbx5) (8). Loss of SRC-2 results in extensive cardiac transcriptional remodeling, leading to a gene landscape that resembles the fetal gene profile during unstressed conditions, but with no corresponding impairment of function (9). During pressure overload induced by TAC, SRC-2 KO animals have an abrogated hypertrophic response and decreased sustained cardiac function compared with WT animals (9). In the current study, we show that mice with loss of SRC-2 in the cardiomyocyte (SRC-2 CKO) have a similar impaired response to TAC.

Investigation of this model revealed a novel role for SRC-2 as a regulator of paracrine signaling from the cardiomyocyte. We found that SRC-2 CKO hearts have reduced vasculature in response to TAC, which at least partially results from decreased VEGF secretion from the cardiomyocytes. *In vitro* studies revealed that SRC-2 coactivates both GATA-4 and HIF transcription factors to induce VEGF expression and secretion in response to hypertrophic and hypoxic stimuli. Together, our results suggest that SRC-2 is a novel upstream coordinator of cardiomyocyte-driven angiogenesis during cardiac stress, bridging both hypertrophic and hypoxic-stimulated paracrine signaling.

Results

Cardiomyocyte SRC-2 absence prevents TAC-induced increased cardiac vasculature

To analyze cardiomyocyte-specific activities of SRC-2 during cardiac stress, we subjected WT and SRC-2 CKO mice to TAC and monitored their cardiac function for 4 weeks. Similar to what we observed previously for universal SRC-2 KO animals (9), loss of cardiomyocyte SRC-2 resulted in blunted hypertrophy, as measured by left ventricular wall thickness and cardiomyocyte size, and decreased function, as measured by ejection fraction and fractional shortening compared with WT mice (Fig. 1, *A–C*). Mice were euthanized 4 weeks post-TAC because of accelerated heart failure in the SRC-2 CKO mice. Because hypertrophy acutely promotes angiogenesis, which in turn can support further hypertrophy, we postulated that a lack of angiogenic response could impair the degree of hypertrophy in SRC-2 CKO mice as well as contribute to the observed

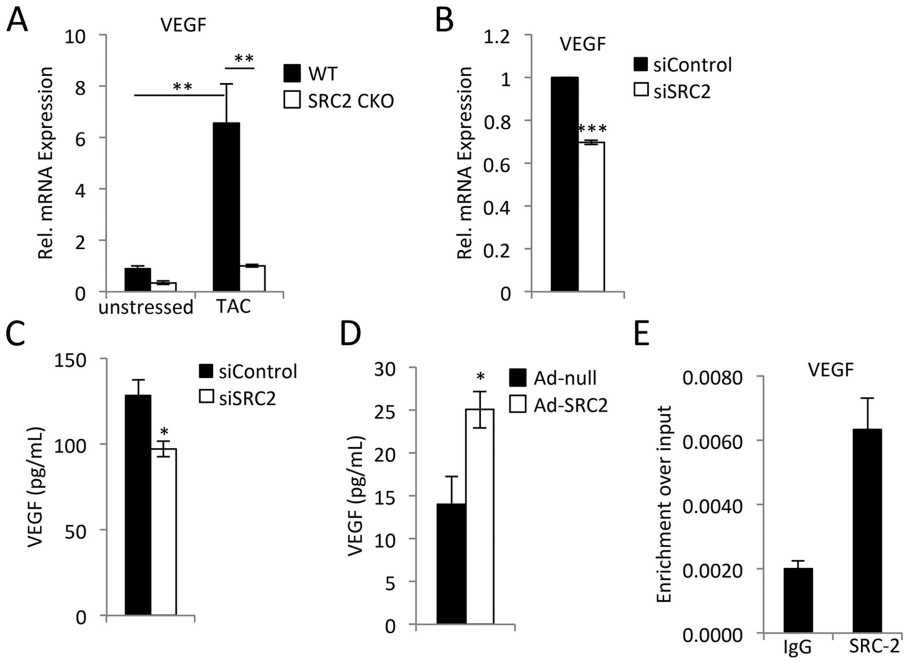

Figure 2. SRC-2 promotes VEGF expression and secretion from cardiomyocytes. *A*, qPCR for VEGF expression in total heart RNA from WT and SRC-2 CKO hearts before and 4 weeks after TAC. Rpl32 is used as an internal control, and data are presented relative to unstressed WT. $n = 4$. *B*, qPCR for VEGF in total RNA from H9c2 cells treated with control or SRC-2 siRNA. Rpl32 is used as an internal control, and data are presented relative to control siRNA. *C*, ELISA analysis for VEGF in medium collected from H9c2 cells treated with control or siRNA against SRC-2. *D*, ELISA as described in *C* from H9c2 cells treated with control empty adenovirus or ad-SRC2. *E*, chromatin immunoprecipitation performed with anti-SRC-2 antibodies in total chromatin prepared from adult primary cardiomyocytes and analyzed for enrichment of the VEGF promoter via qPCR. IgG antibodies are used as negative controls. A primer set known to be void of SRC-2 binding was used as a control, and enrichment was too low to amplify in qPCR. *, $p \leq 0.05$; **, $p \leq 0.01$; ***, $p \leq 0.001$. *Error bars*, S.E.

decreased function. Isolectin staining of heart sections 4 weeks post-TAC revealed increased vasculature in the WT animals. In contrast, the vasculature in the SRC-2 CKO mice did not increase but actually slightly decreased (Fig. 1*D*). This impaired vasculogenesis post-TAC accompanies decreased mRNA expression of endothelial markers Tie2, CD31, and TAC1 in SRC-2 CKO animals compared with WT post-TAC (Fig. 1*E*). These results strongly suggest that loss of SRC-2 in the cardiomyocyte prevents the angiogenic response to pressure overload.

SRC-2 promotes VEGF expression and secretion

Of the many factors secreted from cardiomyocytes that can affect angiogenesis during stress, VEGF is most predominant (1). The expression of VEGF induced by TAC was greatly blunted in SRC-2 CKO animals (Fig. 2*A*). To ensure that this effect is not due to developmental loss of SRC-2, we tested acute knockdown of SRC-2 in H9c2 rat cardiomyocytes and found that a similar decrease in VEGF mRNA expression accompanies decreased SRC-2 expression (Fig. 2*B* and Fig. S1*A*). Additionally, knockdown of SRC-2 in H9c2 cells reduced their secretion of VEGF (Fig. 2*C*). By contrast, increased expression of SRC-2 via adenovirus augmented VEGF secretion (Fig. 2*D*). Chromatin immunoprecipitation assays confirmed SRC-2 recruitment to the VEGF promoter in isolated primary adult cardiomyocytes (Fig. 2*E*). These data support the idea that SRC-2 up-regulates VEGF expression in the cardiomyocyte.

Induction of VEGF by SRC-2 promotes angiogenesis in endothelial cells in vitro

VEGF secretion from cardiomyocytes stimulates angiogenesis, a process that involves EC proliferation, migration, and tube formation (1). To investigate whether SRC-2 played a role in this paracrine effect of cardiomyocytes, we assessed the effects of conditioned media from WT and SRC-2–deficient H9c2 cardiomyocytes. Conditioned medium from SRC-2 knockdown cardiomyocytes stimulated less HUVEC tube formation and proliferation. This impairment was rescued with the addition of exogenous VEGF to the medium (Fig. 3, *A* and *B*). Conversely, HUVEC proliferation was augmented to a greater extent using conditioned medium from SRC-2–overexpressing cardiomyocytes (Fig. 3*C*). These data suggest that SRC-2 regulates the paracrine effect of cardiomyocytes on angiogenesis.

Angiotensin II (AngII) stimulates SRC-2 expression and VEGF expression in an SRC-2–dependent manner

The earliest signals driving angiogenesis downstream of pressure overload are initiated by hypertrophic signaling (1). Little is known about control of SRC-2 expression and activity in the heart in response to stress or growth signals, so we investigated whether hypertrophic signals might induce SRC-2 activity and whether this activity would lead to increased VEGF expression. SRC-2 mRNA and protein levels were increased in H9c2 cardiomyocytes in response to hypertrophic agonist AngII (Fig. 4*A*). We recently generated a mouse line with inducible loss of SRC-2 specifically in the cardiomyocyte in response to

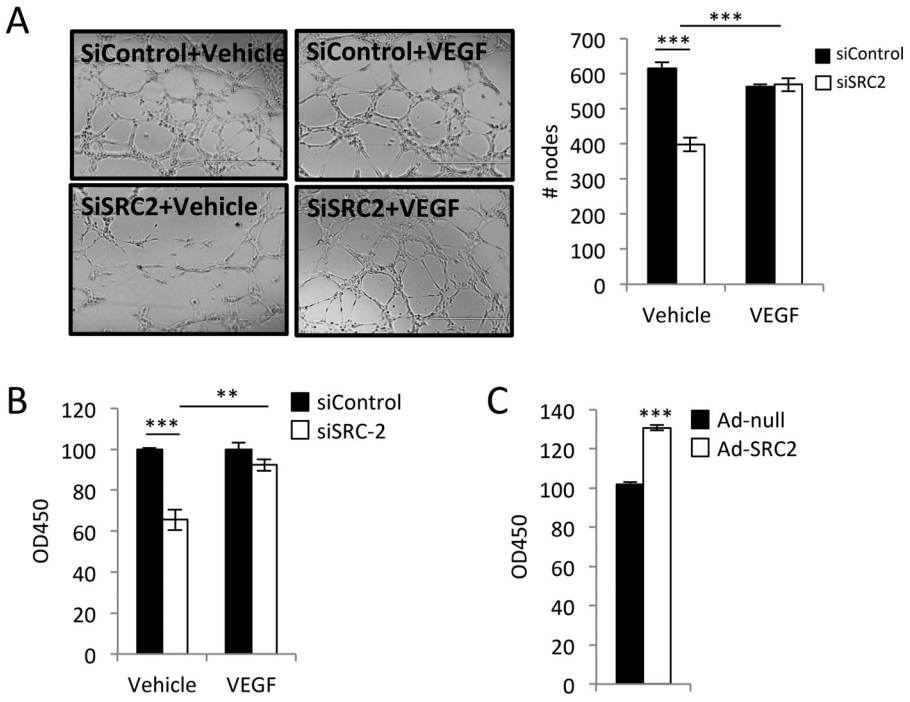

Figure 3. SRC-2-induced paracrine VEGF release from cardiomyocytes is sufficient to promote endothelial cell activation. *A*, tube formation assays in HUVECs performed in conditioned medium from H9c2 cells treated with control or siRNA against SRC-2. This medium was supplemented with vehicle or exogenous VEGF, as indicated. *B*, HUVEC proliferation measured by XTT assays using conditioned medium as described in *A*. *C*, HUVEC proliferation measured by XTT assays using conditioned medium from H9c2 cells infected with control empty adenovirus or Ad-SRC2. **, $p \leq 0.01$; ***, $p \leq 0.001$. *Error bars*, S.E.

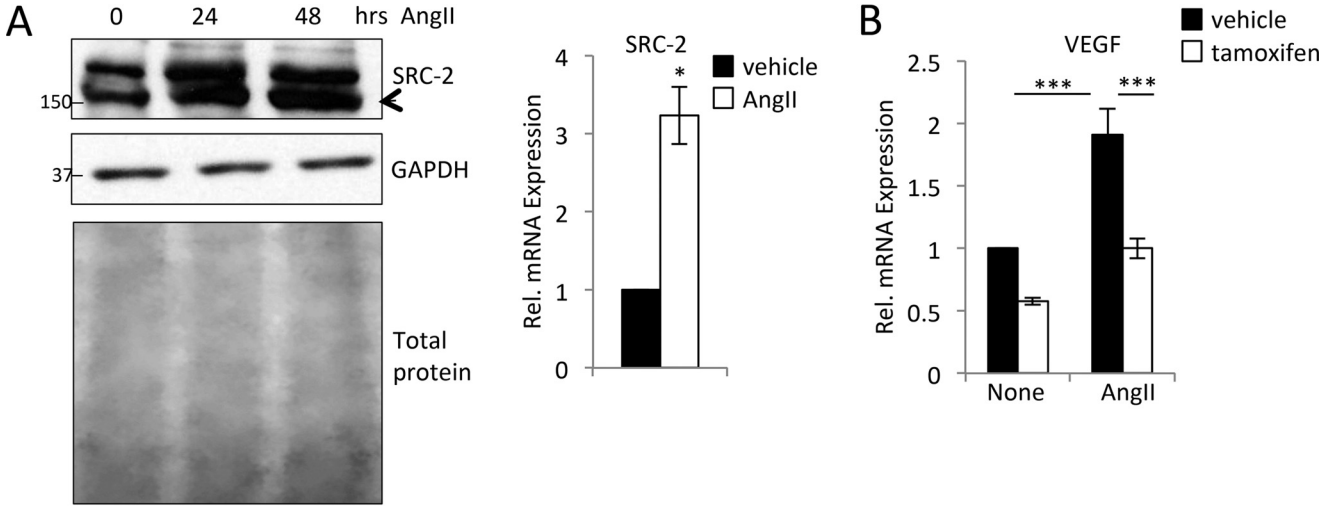

Figure 4. AngII induces SRC-2 and VEGF expression. *A*, immunoblotting for SRC-2 in H9c2 cells treated with AngII for the indicated times. GAPDH and total protein are used as loading controls. qPCR for SRC-2 was performed in H9c2 cells treated with AngII for 24 h. Rpl32 was used as in internal control, and data are presented relative to vehicle. *B*, qPCR for VEGF from isolated adult cardiomyocytes from mice treated with vehicle or tamoxifen to induce knockout of SRC-2. After isolation, cardiomyocytes were treated with vehicle or AngII for 12 h. Rpl32 was used as an internal control, and data are presented relative to vehicle control. Data are presented relative to vehicle control. *, $p \leq 0.05$; ***, $p \leq 0.001$. *Error bars*, S.E.

tamoxifen injection (Fig. S1*B*). In vehicle- or AngII-treated adult primary cardiomyocytes isolated from these mice injected with vehicle or tamoxifen, decreased SRC-2 resulted in decreased VEGF mRNA expression (Fig. 4*B*). There was no significant effect of SRC-2 knockdown on hypertrophic gene expression in either cell type (Fig. S1).

SRC-2 coactivates GATA-4 to induce VEGF expression

GATA-4 is a potent inducer of VEGF downstream of TAC (3), and we have previously shown that SRC-2 coactivates GATA-4 in the heart (8). Together, these data suggest coordinated activation of VEGF by SRC-2 and GATA-4 (Fig. 5*A*). To test this hypothesis, we obtained the proximal promoter of VEGF with WT and mutated GATA-4–binding sites (3) and assessed transactivation in the presence of GATA-4 and SRC-2. SRC-2 alone increased expression of the VEGF proximal promoter and coactivated GATA-4 expression on the WT promoter (Fig. 5*B*). When the two main GATA-4 sites were mutated, reporter activity was substantially decreased, suggest-

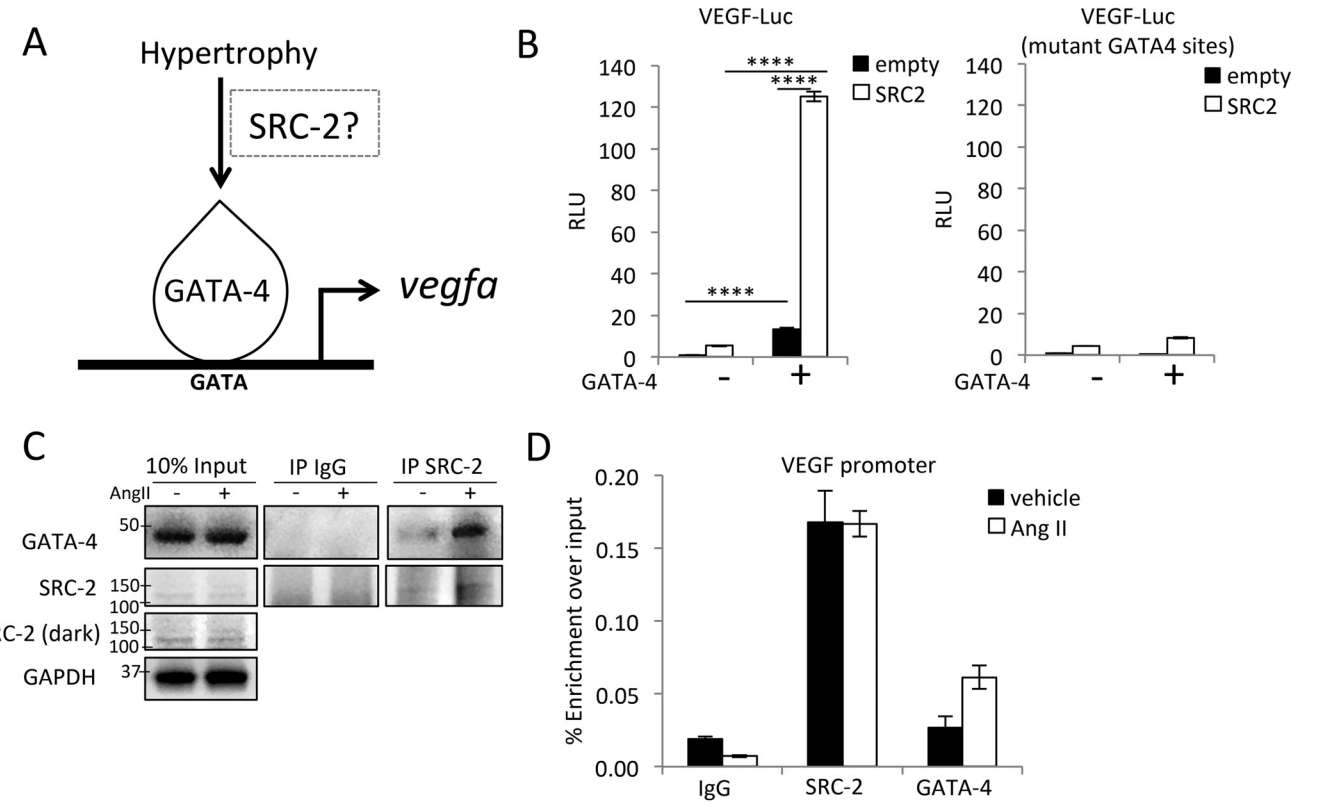

Figure 5. SRC-2 promotes VEGF expression through GATA-4. *A*, schematic of hypertrophic induction of VEGF suggesting a possible role for SRC-2 in mediating signal-dependent activation of VEGF by GATA-4. *B*, luciferase transactivation assays in H9c2 cells with the −1300 to +1 fragment of the VEGF proximal promoter. *mutant GATA-4 sites*, a promoter with mutations of the GATA-4–binding sites. SRC-2 and GATA-4 were transiently overexpressed from plasmids where indicated. *C*, co-immunoprecipitation experiments using anti-SRC-2 or IgG (control) antibodies in lysates from H9c2 cells treated with vehicle or AngII for 12 h and analyzed for expression with the indicated antibodies. GAPDH is used as a loading control for input. *D*, chromatin immunoprecipitation experiments with the indicated antibodies performed in total chromatin-prepared H9c2 cells treated with vehicle or AngII for 12 h and analyzed for enrichment of the VEGF promoter via qPCR. IgG antibodies were used as negative controls. A primer set known to be void of SRC-2 binding was used as a control, and enrichment was too low to amplify in qPCR. ****, $p < 0.0001$. *Error bars*, S.E.

ing that SRC-2 coactivation is largely mediated through these sites (Fig. 5*B*). Furthermore, AngII treatment of H9c2 cells increased the interaction between SRC-2 and GATA-4 (Fig. 5*C*), and both SRC-2 and GATA-4 were located at the VEGF promoter during AngII treatment of H9c2 cells (Fig. 5*D*). These results suggest that hypertrophic signals can increase SRC-2 expression and further enhance VEGF expression through increased coactivation of GATA-4 in cardiomyocytes.

SRC-2 is induced by hypoxia in the cardiomyocyte via HIF transactivation

The second major physiological signal driving angiogenesis in response to TAC is hypoxia. In theory, inhibition of hypertrophic induction of angiogenesis would accelerate hypoxia in the myocardium; however, hypoxia could rescue this defect through induction of angiogenesis by another mechanism. The degree of impairment of TAC-induced angiogenesis in SRC-2 CKO hearts (Fig. 1) suggests that SRC-2 also controls this secondary mechanism of angiogenesis. In this case, we would expect SRC-2 activity to also be induced by hypoxic signals. Incubation of isolated adult cardiomyocytes with cobalt chloride ($CoCl_2$) to mimic hypoxia leads to robust induction of SRC-2 mRNA (Fig. 6*A*). Incubation of H9c2 cardiomyocytes under hypoxic conditions also resulted in increased SRC-2 mRNA and protein expression, albeit under different kinetics (Fig. 6, *B* and *C*). Additionally, SRC-2 mRNA increased in hearts from mice incubated in a hypoxic chamber for 7 days compared with normoxic conditions (Fig. 6*D*). To test whether these effects on SRC-2 expression are through direct transcriptional control, we performed transactivation assays in H9c2 cardiomyocytes stably expressing the SRC-2 proximal promoter incubated with either $CoCl_2$ or 1% O_2. In support of direct transcriptional activation of SRC-2, both treatments increased activation of the promoter (Fig. 6*E*). Furthermore, we found four consensus hypoxia response elements in this promoter region and show that both HIF-1α and HIF-2α can activate the SRC-2 proximal promoter (Fig. 6*F*). Both HIFs were also recruited to the SRC-2 promoter in H9c2 cells treated with $CoCl_2$ (Fig. 6*G*). Together, these data indicate that hypoxia induces SRC-2 expression.

SRC-2 coactivates HIFs to induce VEGF expression under hypoxia

VEGF induction in response to hypoxia is largely driven through HIF-1α and -2α (Fig. 7*A*). We therefore tested whether SRC-2 coactivates HIF-1α and HIF-2α in cardiomyocytes. We found that SRC-2 interacted with HIFs in hypoxic mouse heart lysates (Fig. 7*B*). Additionally, SRC-2 coactivated HIFs to increase activity of the VEGF proximal promoter in H9c2 cardiomyocytes (Fig. 7*C*). Similarly, knockdown of SRC-2 expres-

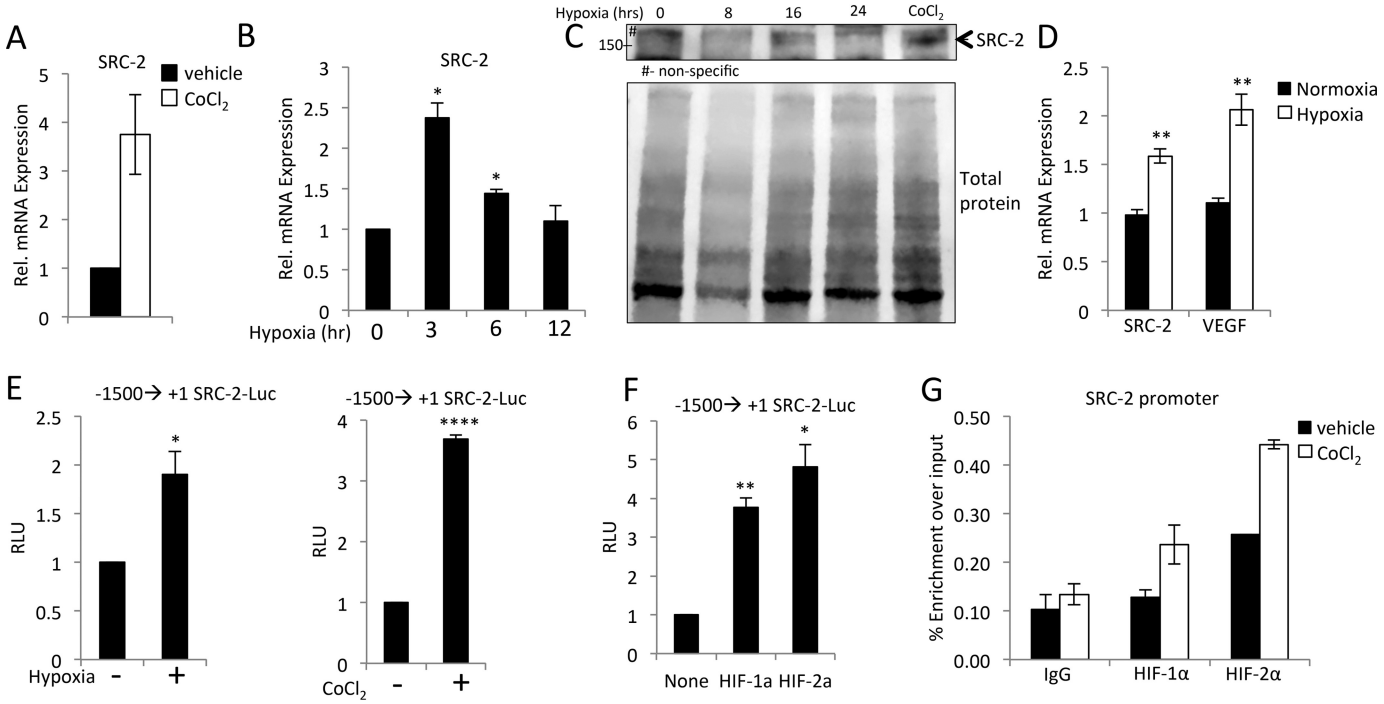

Figure 6. Hypoxia induces SRC-2 expression. *A*, qPCR for SRC-2 in isolated adult cardiomyocytes treated with vehicle or $CoCl_2$ for 12 h to mimic hypoxia. Rpl32 was used as an internal control, and data are presented relative to vehicle control. *B*, qPCR for SRC-2 in H9c2 cells cultured under hypoxic conditions for the indicated times. Rpl32 was used as an internal control, and data are presented relative to normal oxygen conditions. *C*, immunoblotting with SRC-2 antibodies or total protein staining in whole-cell lysates from H9c2 cells grown in 1% O_2 for the indicated times. *Arrows*, SRC-2 band. *D*, qPCR for SRC-2 and VEGF in total heart RNA isolated from mice incubated under normoxic or hypoxic gas for 7 days. Rpl32 was used as an internal control, and data are presented relative to expression under normoxia for each gene independently. *E*, luciferase assays in H9c2 cells stably transfected with −1500 to +1 of the SRC-2 proximal promoter treated with hypoxic gas or $CoCl_2$ for 24 h as indicated. *F*, luciferase assays in H9c2 cells −1500 to +1 of the SRC-2 proximal promoter with plasmid-driven overexpression of HIF-1α and HIF-2α as indicated. Data are presented relative to promoter alone. *G*, chromatin immunoprecipitation experiments with the indicated antibodies performed in total chromatin-prepared H9c2 cells treated with or without $CoCl_2$ for 12 h and analyzed for enrichment of the SRC-2 promoter via qPCR. IgG antibodies are used as negative controls. A primer set known to be void of SRC-2 binding was used as a control, and enrichment was too low to amplify in qPCR. *, $p \leq 0.05$; **, $p \leq 0.01$; ****, $p < 0.0001$. *Error bars*, S.E.

sion in H9c2 cardiomyocytes resulted in decreased VEGF expression during hypoxia (Fig. 7*D*), and decreased cardiomyocyte SRC-2 suppressed VEGF expression in isolated primary adult cardiomyocytes treated with $CoCl_2$ (Fig. 7*E*). $CoCl_2$-induced VEGF secretion from H9c2 cells was also impaired by knockdown of SRC-2 (Fig. 7*F*). Last, SRC-2, HIF-1α, and HIF-2α were recruited to the VEGF promoter in $CoCl_2$-treated H9c2 cells (Fig. 7*G*). Combined, these data support the hypothesis that SRC-2 and HIF-1α and -2α work in a feed-forward loop to induce VEGF expression in hypoxic cardiomyocytes.

Discussion

In this work, we present a novel regulator of cardiomyocyte-induced angiogenesis, SRC-2, which we postulate induces VEGF expression from both hypertrophic and hypoxic signaling pathways (Fig. 8). The novel contributions include the following. 1) SRC-2 controls VEGF expression and secretion from cardiomyocytes through both GATA-4 and HIFs. 2) SRC-2 expression is stimulated by both hypertrophic and hypoxic signals in the heart. 3) Loss of SRC-2 impairs TAC-induced angiogenesis *in vivo*. Our results further support the idea that SRC-2 is a major upstream coordinator of the cardiac transcriptional response to stress.

The decreased VEGF correlates strongly with decreased vasculature post-TAC in SRC-2 CKO hearts compared with WT hearts, which is expected to contribute to the decline in cardiac function observed in these animals. These observations are strongly supported by several studies showing the detrimental effects of decreased angiogenic capabilities on cardiac function in response to TAC, including those describing HIF and GATA-4 control of angiogenesis (3, 5). Therefore, although it is probably not the only mechanism disrupted by loss of SRC-2 that results in cardiac decline during pressure overload, loss of vasculature during cardiac stress is probably a major contributor to this phenotype. Because of the close relationship between hypertrophy and angiogenesis and possible roles for SRC-2 in both mechanisms, we cannot currently definitely rule out that the decreased vasculature *in vivo* in SRC-2 CKO hearts results from a decreased need for angiogenesis because SRC-2 CKO hearts have decreased hypertrophy. However, our *in vitro* data strongly support a direct role for SRC-2 in regulation of VEGF expression, suggesting that this mechanism contributes to the overall *in vivo* phenotypes observed.

Previously, we have shown that SRC-2 can control metabolic, sarcomeric, and stress-responsive genes in the heart by interacting with several transcription factors, including peroxisome proliferator–activated receptor α (PPARα), GATA-4, MEF2, and Tbx5 (8). In this report, we extend the role of SRC-2 in controlling cardiomyocyte function and activity and for the first time describe a stress signal– dependent activity for SRC-2 in the heart. It is important to note that as a coactivator, SRC-2

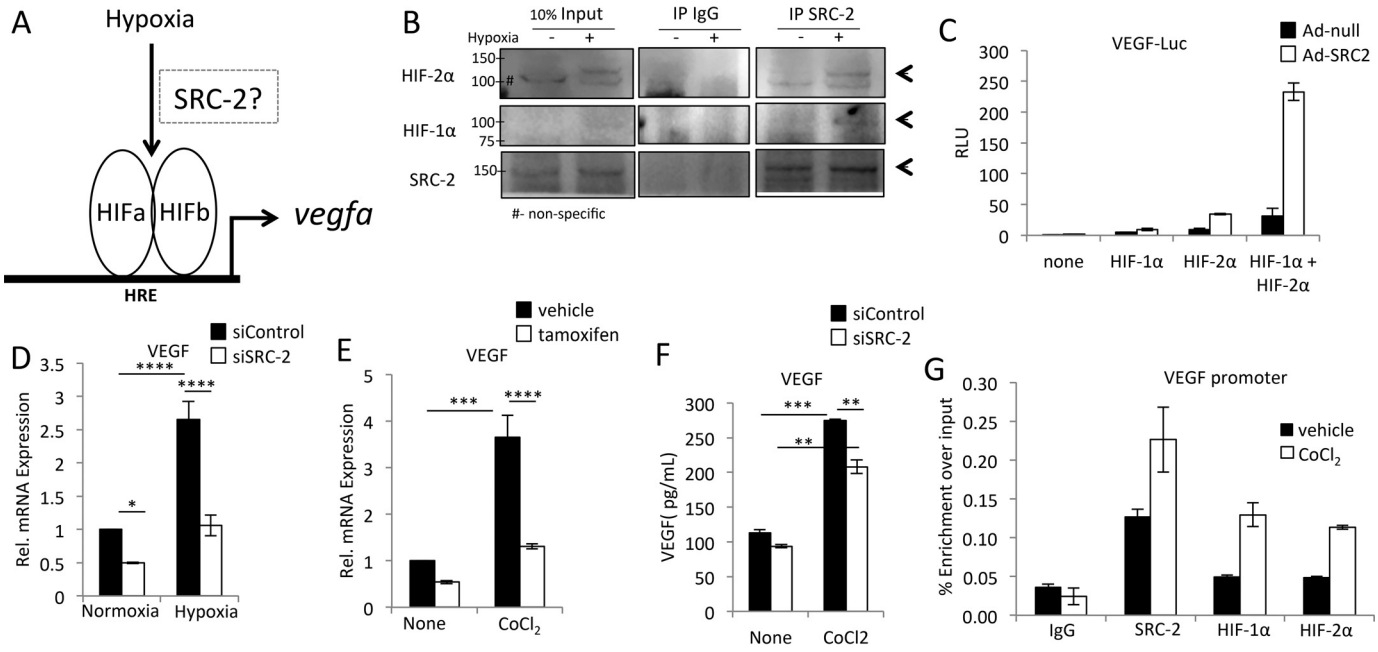

Figure 7. SRC-2 coactivates HIFs to increase hypoxia-induced VEGF expression. *A*, schematic of hypoxic induction of VEGF, suggesting a possible role for SRC-2 in mediating signal-dependent activation of VEGF by HIFs. *B*, co-immunoprecipitation experiments in whole-heart lysates from mice housed under normoxia or hypoxia for 7 days using anti-SRC-2 or IgG (control) antibodies and analyzed for expression with the indicated antibodies. Equal protein concentration was added in each *lane*. *Arrows*, target bands. *C*, luciferase assays in H9c2 cells of the −1300 to +1 VEGF proximal promoter with empty adenovirus or Ad-SRC-2 and plasmid-driven overexpression of HIF-1α and HIF-2α, as indicated. *D*, qPCR for VEGF in total RNA from H9c2 cells treated with control or SRC-2 siRNA and hypoxic conditions, as indicated. Rpl32 was used as an internal control, and data are presented relative to control siRNA under normoxic conditions. *E*, qPCR for VEGF from isolated adult cardiomyocytes from mice treated with vehicle or tamoxifen to induce knockout of SRC-2. After isolation, cardiomyocytes were treated with vehicle or $CoCl_2$ for 12 h. Rpl32 is used as an internal control, and data are presented relative to vehicle control. Data are presented relative to vehicle control. *F*, ELISA for VEGF in medium collected from H9c2 cells treated with control or siRNA against SRC-2 and $CoCl_2$ for 24 h, as indicated. *G*, chromatin immunoprecipitation experiments with the indicated antibodies performed in total chromatin-prepared H9c2 cells treated with or without $CoCl_2$ for 12 h and analyzed for enrichment of the VEGF promoter via qPCR. IgG antibodies are used as negative controls. A primer set known to be void of SRC-2 binding was used as a control, and enrichment was too low to amplify in qPCR. *, $p \leq 0.05$; **, $p \leq 0.01$; ***, $p \leq 0.001$; ****, $p < 0.0001$. *Error bars*, S.E.

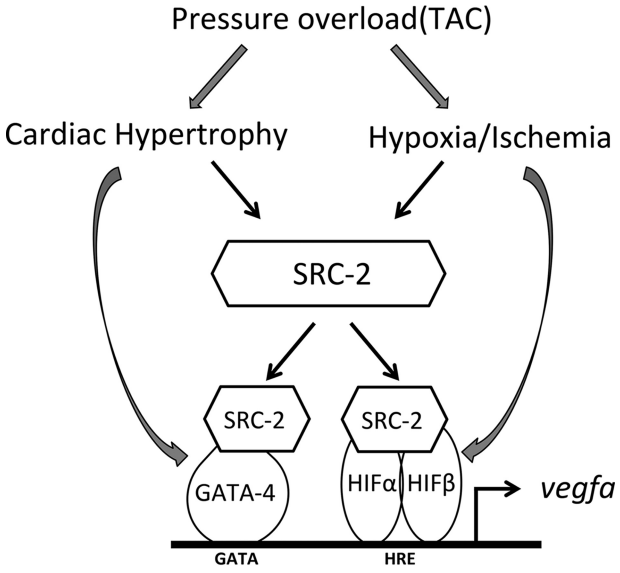

Figure 8. Model of SRC-2 control of cardiomyocyte VEGF. In cardiomyocytes subject to pressure overload, hypertrophic signals lead to both increased SRC-2 and activation of GATA-4. SRC-2 can coactivate GATA-4 to drive VEGF expression and secretion from the cardiomyocyte. Pressure overload can also lead to hypoxic activation of HIF2 in the cardiomyocyte that can lead to increased SRC-2 that positively feeds forward to coactivate HIFs to further increase VEGF expression and secretion. The secreted VEGF can then stimulate endothelial cells to drive angiogenesis.

is not required for transcription factor binding to the DNA but is an important component of the recruitment of coactivator complexes and the general transcription machinery that lead to induction and/or amplification of the target gene. We show that SRC-2 is increased in cardiomyocytes through both hypertrophic and hypoxic signals and can integrate these two signals to drive a single response, VEGF expression. This is among the first reports showing direct control of release of a paracrine factor by SRC-2. Whereas hypoxic induction of SRC-2 expression appears to be, at least in part, mediated by HIFs themselves, hypertrophic control of SRC-2 expression may be partially transcription-regulated but is amplified post-transcriptionally. Interestingly, AngII treatment increased the association between SRC-2 and GATA-4. We currently do not know whether this is due to increased phosphorylation and activation of GATA-4, as has been described previously (10, 11); a possible unknown post-translational modification of SRC-2; or perhaps changes in localization of another factor important for bridging or strengthening this association. Understanding the dynamics of this association may be important in further defining the mechanisms of GATA-4 gene targeting and activation during different stages of the stress response. Furthermore, this is a novel description of a regulator that is poised to coordinately control the hypertrophy–hypoxia angiogenic axis in cardiomyocytes, which has previously been hypothesized to exist but remains uncharacterized (2).

Herein, we describe coordinate control of VEGF expression via SRC-2 coactivation of GATA-4 and HIFs, in response to hypertrophic and hypoxic signals, respectively. Our data do not exclude possible contribution of these factors in the corre-

sponding pathways, and indeed, GATA-4 has been shown to increase during hypoxia to the right ventricle (12) as well as to undergo direct control by miR-26b, which is reduced by hypoxia in the myocardium and, therefore, would increase GATA-4 expression (13). Furthermore, both HIF-1α and -2α are potently induced by hypoxia but can increase in some circumstances due to growth factor signaling (14). Therefore, cross-talk between these mechanisms is not unlikely and may point further toward SRC-2 acting as a major scaffolding protein to bridge between multiple environmental and timing signals to drive a single response. Additionally, these are not the only transcription factors known to activate VEGF in response to various stimuli. Mutation of the GATA-4–binding sites in the VEGF proximal promoter largely decreased, but did not fully ablate, SRC-2 coactivation of this region, suggesting other contributors to VEGF expression with which SRC-2 may coordinate. Others include signal transducer and activator of transcription 3 (Stat3) and PPARγ (15, 16), which may also be controlled by SRC-2 in the cardiomyocyte (8); however, signal and target-dependent regulation of these dynamics has not been investigated. Peroxisome proliferator activated receptor γ coactivator-1α (PGC-1α) coactivates estrogen-related receptor α (ERRα) through binding sites in this same region in skeletal muscle cells (17). We have previously shown that SRC-2 deficiency in the heart results in decreased PGC-1α expression (9), but whether PGC-1α controls VEGF in the heart is currently unknown. MEF2, which we have previously shown associates with SRC-2 in cardiomyocytes, also binds to an upstream enhancer in the VEGF promoter in endothelial cells (18). Although we did not observe any AngII–dependent increases in MEF-2– or SRC-2–driven transcription from this region (data not shown), we currently cannot rule out a possible additive role for this mechanism during hypertrophy *in vivo*. Expression of VEGF expression is tightly controlled and downstream of several distinct signaling pathways. We support the notion that there is SRC-2–independent control of VEGF as well as other unidentified SRC-2-dependent control mechanisms.

Experimental procedures

Animals

All animal experiments were approved by the Institutional Animal Care Research Committee at Houston Methodist Research Institute or Baylor College of Medicine. SRC-2 CKO animals have been described previously and have loss of SRC-2 specifically in cardiomyocytes, as Cre expression is under the control of the Myh6 promoter (Fig. S2) (8). Mice with inducible knockout of cardiomyocyte SRC-2 were generated by crossing SRC-$2^{f/f}$ mice with transgenic mice with Myh6-Cre/Esr1 promoter (Jackson Laboratory). A single 40-mg/kg tamoxifen injection was used to induce Cre expression 2 months before harvest. Under these conditions, SRC-2 expression was lost in ~60% of cardiomyocytes (Fig. S1*B*). Hypoxia studies were performed on ICR wild-type mice left in normoxia or placed in a hypoxic chamber at 10.5% oxygen for 7 days before harvest.

Plasmids and reagents

The pCR3.1-SRC-2 plasmid has been described previously (19). The pCGN-GATA-4 was a gift from Dr. Mona Nemer (20). pVEGF-Luc was a gift from Dr. Jeffery D. Molkentin (3). HA-HIF-1α-pcDNA3 and HA-HIF-2α-pcDNA3 were a gift from William Kaelin (Addgene) (21). Adenovirus containing GFP and GFP-Cre recombinase (Ad5-CMV-GFP and Ad5-CMV-Cre-GFP, respectively) were purchased from the Vector Development Core at Baylor College of Medicine. pAdeno-SRC-2 has been described previously (8). siRNAs against SRC-2 were purchased from Dharmacon.

Cell culture

H9c2 (ATCC) and HUVEC (LONZA) were cultured by standard methods according to the suppliers' instructions. Treatments were performed as indicated with the following parameters. $CoCl_2$ was used at a concentration of 200 μM for 12 or 24 h, and AngII was used at a concentration of 1 μM for 12 or 24 h. Hypoxic cultures were performed either in an incubator with oxygen regulator at 1% O_2, 94% N_2, and 5% CO_2 (BioSpherix) or in a modular hypoxic chamber (Billups–Rothenberg) filled with premixed gas at 1% O_2, 5% CO_2, and 95% N_2. All experiments with cells were repeated a minimum of three times to ensure reproducibility of experimental trends.

siRNA-mediated knockdown

H9c2 cells were transfected with Lipofectamine 3000 at a density of 1×10^7 cells/ml with 100 μM siRNA according to the manufacturer's instructions (Thermo Fisher Scientific). Cells were treated as described and harvested 48 h later. Under these conditions, SRC-2 expression is decreased by about 50% (Fig. S1*A*).

Gene expression analyses

RNA was isolated from either cells or frozen heart tissue using the RNeasy RNA isolation kit or fibrous tissue kit, respectively, according to the manufacturer's instructions (Qiagen). cDNA analysis was performed on 500–1000 ng of RNA using random primers and the iScript enzyme according to the manufacturer's instructions (Bio-Rad). qPCR analyses were performed using Quanta SYBR Green (Quanta Bio) on a Roche light cycler qPCR machine. Primer sequences are available upon request.

Aortic constriction and cardiac measurements

Transverse aortic banding was performed as described previously (22). Echocardiography and Doppler measurements were made as described previously (22–24). Twenty-four hours after surgery, the flow velocity of the right and left carotids is assessed via Doppler, the ratio of which provides a measurement of the severity of constriction. This ratio was statistically similar in all groups (Fig. S3). All mice were injected with saline once daily for 6 days before experimentation. Echocardiography and Doppler measurements were taken at pre-TAC and at 1-, 2-, and 4-week intervals. Four weeks after TAC, animals were euthanized, and hearts were immediately removed. Transverse sections were cut and immediately fixed in Z-fix for

paraffin embedding, and the rest of the heart was minced and snap-frozen in liquid nitrogen. Animal numbers were chosen based on power analysis before banding was performed; however, this procedure causes some lethality, so final group sizes were as follows (pre-TAC, 1-week, 2-week, and 4-week): WT, 15, 11, 10, and 10; SRC-2 CKO, 12, 9, 9, and 7. Data were excluded from analysis when images inhibited accurate measurements of all parameters. Banding and analysis were performed in three independent groups of littermate mice, and personnel performing surgery, echocardiography, and Doppler measurements were blinded to their genotype. Each surgical group contained littermates, and all male mice from each litter were used to avoid bias.

Adult cardiomyocyte isolation

Adult cardiomyocytes were isolated as described previously (25). Briefly, aortas of freshly isolated hearts were cannulated and perfused with type IV collagenase (Gibco) followed by mincing and calcium reintroduction. Cardiomyocytes from several mice were pooled, plated, and finally cultured at 2% CO_2 in media containing ITS medium supplement and 2,3-butanedione monoxime.

Chromatin immunoprecipitation

H9c2 cells or freshly isolated primary cardiomyocytes were immediately fixed for 10 min with 1% formaldehyde, and downstream analyses were performed with the SimpleChip enzymatic chromatin IP kit (Cell Signaling Technology). Each immunoprecipitation was conducted with 3 μg of antibody. Beads and antibody were preincubated in 0.5% bovine serum albumin in 1× PBS overnight before the addition of chromatin. Final products were eluted in 50 μl. qPCR analysis was performed with SYBR Green and gene-specific primers on a Roche light cycler. Antibodies used were as follows: anti-SRC-2 (A300-346A, Bethyl Laboratories), anti-GATA (H-112, Santa Cruz Biotechnology), anti-HIF-1α (NB100-105, Novus), and anti-HIF-2α (NB100-122, Novus). Primer sequences were as follows: mouse Untr10 (forward, 5′-tacacatgaggcccaggatca-3′; reverse, 5′- tggctccttcagtcctttatg-3′) (negative control; data not shown due to lack of enrichment); mouse VEGF (forward, 5′-cccagctgtctctccttcag-3′; reverse, 5′-tgtggaaacccacgtatgc-3′); rat VEGF (forward, 5′-ctctcttgggtgcactgga-3′; reverse, 5′-cacgaccgcttaccttgg-3′; rat SRC-2 (forward, 5′-cagcagtgacgtgctagtgaa-3′; reverse, 5′-catccatagcagaggcaagg-3′).

Immunoprecipitation

H9c2 cells were treated as indicated before harvest. Cells were lysed in RIPA buffer (1× PBS, 1% Nonidet P-40, 0.5% sodium deoxycholate, 0.1% SDS) plus protease inhibitors. The resulting lysates were incubated with the indicated antibodies and protein A/G Dynabeads (Thermo Fisher Scientific) for 3 h in RIPA buffer with protease inhibitors at 4 °C. Immunoprecipitates were washed and analyzed via SDS-PAGE. The products were visualized with anti-HRP conjugates and ECL detection (EMD Millipore). Antibodies used to immunoprecipitate were anti-SRC-2 (A300-346A, Bethyl Laboratories).

Western blotting

H9c2 cells were treated as described and lysed in RIPA buffer plus protease inhibitors. Equal amounts of protein were loaded in wells of the same gel as quantified with a Nanodrop. Proteins were separated via SDS-PAGE and transferred to PVDF membranes. Membranes were blocked and incubated with primary and HRP-conjugated secondary antibodies in 5% milk in 1× Tris-buffered saline + 0.01% Tween 20 (TBST). Proteins were visualized with ECL detection (EMD Millipore) on a LI-COR FC imager (LI-COR). Antibodies used were anti-SRC-2 (A300-345A, Bethyl Laboratories; sc-81280, Santa Cruz Biotechnology), anti-GATA (G-4, Santa Cruz Biotechnology), anti-HIF-1α (NB100-105, Novus), and anti-GAPDH (14C10, Cell Signaling). Total protein staining was performed according to the manufacturer's instructions with REVERT total protein stain (LI-COR).

Isolectin staining

Isolectin staining was performed on deparrafinized heart sections by standard techniques. Blocking was performed in 5% BSA, 10% normal horse serum, and 0.025% Triton X-100 in 1× Tris-buffered saline (TBS) for 2 h at room temperature. Antigen retrieval was performed with Tris-EDTA buffer (10 mM Tris base, 1 mM EDTA solution, 0.05% Tween 20, pH 9.0). Biotinylated isolectin GS-IB_4 (Thermo Fisher Scientific) was used at a concentration of 1:50 at 4 °C overnight in 1× TBS + 1% BSA. After washing with 1× TBS + 0.025% Triton X-100, sections were incubated with Streptavidin-647 (Thermo Fisher Scientific) at a concentration of 1:1000 for 30 min at room temperature in 1× TBS + 1% BSA. Autofluorescence was blocked using 0.1% Sudan Black B in 70% ethanol for 30 min at room temperature. Sections were dehydrated and mounted with Vectashield mounting medium containing DAPI (Vector Laboratories). Imaging was performed with a Cy5 filter on an EVOS FL microscope (Thermo Fisher Scientific).

ELISA

ELISAs for VEGF were performed on medium collected from H9c2 cells treated as described using a rat VEGF ELISA kit according to the manufacturer's instructions (Sigma).

Tube formation

H9c2 cells were treated with scrambled si or siSRC-2 (Dharmacon) as described above. 48 h later, medium was collected from the wells (conditioned medium). 50 μl of growth factor-reduced Matrigel was incubated in each well of a 96-well plate at 37 °C for 20 min. Then 2.5 × 10^4 HUVECs were loaded in the precoated wells with 100 μl of conditioned medium with or without 600 pg/ml VEGF (Peprotech). Four wells were analyzed per condition, and two pictures of each well were taken for measurements. ImageJ software was used for the measurements.

Cell proliferation assay

HUVEC proliferation was assessed using the XTT cell viability kit according to the manufacturer's instructions (Cell Signaling). Briefly, HUVECs were plated in 96-well plates at 10^4

cells/well and incubated with conditioned medium from H9c2 cells infected with adenovirus expressing null or SRC-2 (Ad-SRC-2) or control or SRC-2 siRNAs. After 48 h, XTT solution was added to each well and incubated for 4–8 h at 37 °C. A_{450} readings correlate with cell number.

Statistical analysis

All data are represented as the means ± S.E. Mean and S.E. were calculated using Excel software (Microsoft Corp.). All comparisons involving two variables were analyzed using Prism software (GraphPad) by 2-way analysis of variance with multiple comparisons. For animal studies, the analysis of variance was calculated with a Sidak post hoc analysis, and for all others, a Tukey post hoc analysis was used. Remaining statistics were performed with a standard Student's *t* test. *, $p \leq 0.05$; **, $p \leq 0.01$; ***, $p \leq 0.001$; ****, $p > 0.0001$.

Author contributions—J. H. S. coordinated the study, analyzed data, and acquired data for all figures. L. L. acquired data related to endothelial cells. D. N. and J. K. acquired *in vitro* cardiomyocyte data and helped with data analysis. J. J. acquired mouse hypoxia data. G. E. T. acquired *in vivo* data and contributed to analysis and interpretation. E. K. helped with *in vitro* experiments and tissue analyses. J. T. K. helped with image analysis and quantitation. H.-K. L. helped in the design and acquisition of *in vivo* hypoxia experiments. M. L. E. and J. P. C. helped with drafting, revision, and study analysis. E. L. R. conceived the study; coordinated all aspects of the study; helped with data acquisition, analysis, and interpretation; and drafted the manuscript. All authors reviewed the results and approved the final version.

Acknowledgments—We thank Hyekyung Park, Hong Chen, Katherina Marcelo, Jennifer Pocius, Thuy Pham, and Alejandro Granillo Ibanez for technical assistance with surgery, cardiac imaging, and molecular analysis.

References

1. Oka, T., Akazawa, H., Naito, A. T., and Komuro, I. (2014) Angiogenesis and cardiac hypertrophy: maintenance of cardiac function and causative roles in heart failure. *Circ. Res.* **114,** 565–571
2. Walsh, K., and Shiojima, I. (2007) Cardiac growth and angiogenesis coordinated by intertissue interactions. *J. Clin. Invest.* **117,** 3176–3179
3. Heineke, J., Auger-Messier, M., Xu, J., Oka, T., Sargent, M. A., York, A., Klevitsky, R., Vaikunth, S., Duncan, S. A., Aronow, B. J., Robbins, J., Cromblehol, T. M., and Molkentin, J. D. (2007) Cardiomyocyte GATA4 functions as a stress-responsive regulator of angiogenesis in the murine heart. *J. Clin. Invest.* **117,** 3198–3210
4. Izumiya, Y., Shiojima, I., Sato, K., Sawyer, D. B., Colucci, W. S., and Walsh, K. (2006) Vascular endothelial growth factor blockade promotes the transition from compensatory cardiac hypertrophy to failure in response to pressure overload. *Hypertension* **47,** 887–893
5. Sano, M., Minamino, T., Toko, H., Miyauchi, H., Orimo, M., Qin, Y., Akazawa, H., Tateno, K., Kayama, Y., Harada, M., Shimizu, I., Asahara, T., Hamada, H., Tomita, S., Molkentin, J. D., *et al.* (2007) p53-induced inhibition of Hif-1 causes cardiac dysfunction during pressure overload. *Nature* **446,** 444–448
6. Bajgelman, M. C., dos Santos, L., Silva, G. J., Nakamuta, J., Sirvente, R. A., Chaves, M., Krieger, J. E., and Strauss, B. E. (2015) Preservation of cardiac function in left ventricle cardiac hypertrophy using an AAV vector which provides VEGF-A expression in response to p53. *Virology* **476,** 106–114
7. Guo, J., Mihic, A., Wu, J., Zhang, Y., Singh, K., Dhingra, S., Weisel, R. D., and Li, R. K. (2015) Canopy 2 attenuates the transition from compensatory hypertrophy to dilated heart failure in hypertrophic cardiomyopathy. *Eur. Heart J.* **36,** 2530–2540
8. Reineke, E. L., Benham, A., Soibam, B., Stashi, E., Taegtmeyer, H., Entman, M. L., Schwartz, R. J., and O'Malley, B. W. (2014) Steroid receptor coactivator-2 is a dual regulator of cardiac transcription factor function. *J. Biol. Chem.* **289,** 17721–17731
9. Reineke, E. L., York, B., Stashi, E., Chen, X., Tsimelzon, A., Xu, J., Newgard, C. B., Taffet, G. E., Taegtmeyer, H., Entman, M. L., and O'Malley, B. W. (2012) SRC-2 coactivator deficiency decreases functional reserve in response to pressure overload of mouse heart. *PLoS One* **7,** e53395
10. Katanasaka, Y., Suzuki, H., Sunagawa, Y., Hasegawa, K., and Morimoto, T. (2016) Regulation of cardiac transcription factor GATA4 by post-translational modification in cardiomyocyte hypertrophy and heart failure. *Int. Heart J.* **57,** 672–675
11. Liang, Q., Wiese, R. J., Bueno, O. F., Dai, Y. S., Markham, B. E., and Molkentin, J. D. (2001) The transcription factor GATA4 is activated by extracellular signal-regulated kinase 1- and 2-mediated phosphorylation of serine 105 in cardiomyocytes. *Mol. Cell. Biol.* **21,** 7460–7469
12. Park, A. M., Wong, C. M., Jelinkova, L., Liu, L., Nagase, H., and Suzuki, Y. J. (2010) Pulmonary hypertension-induced GATA4 activation in the right ventricle. *Hypertension* **56,** 1145–1151
13. Azzouzi, H. E., Leptidis, S., Doevendans, P. A., and De Windt, L. J. (2015) HypoxamiRs: regulators of cardiac hypoxia and energy metabolism. *Trends Endocrinol. Metab.* **26,** 502–508
14. Demidenko, Z. N., and Blagosklonny, M. V. (2011) The purpose of the HIF-1/PHD feedback loop: to limit mTOR-induced HIF-1α. *Cell Cycle* **10,** 1557–1562
15. Biscetti, F., Gaetani, E., Flex, A., Aprahamian, T., Hopkins, T., Straface, G., Pecorini, G., Stigliano, E., Smith, R. C., Angelini, F., Castellot, J. J., Jr., and Pola, R. (2008) Selective activation of peroxisome proliferator-activated receptor (PPAR)α and PPAR γ induces neoangiogenesis through a vascular endothelial growth factor-dependent mechanism. *Diabetes* **57,** 1394–1404
16. Haghikia, A., Ricke-Hoch, M., Stapel, B., Gorst, I., and Hilfiker-Kleiner, D. (2014) STAT3, a key regulator of cell-to-cell communication in the heart. *Cardiovasc Res.* **102,** 281–289
17. Arany, Z., Foo, S. Y., Ma, Y., Ruas, J. L., Bommi-Reddy, A., Girnun, G., Cooper, M., Laznik, D., Chinsomboon, J., Rangwala, S. M., Baek, K. H., Rosenzweig, A., and Spiegelman, B. M. (2008) HIF-independent regulation of VEGF and angiogenesis by the transcriptional coactivator PGC-1α. *Nature* **451,** 1008–1012
18. Shang, Y., Doan, C. N., Arnold, T. D., Lee, S., Tang, A. A., Reichardt, L. F., and Huang, E. J. (2013) Transcriptional corepressors HIPK1 and HIPK2 control angiogenesis via TGF-β-TAK1-dependent mechanism. *PLos Biol.* **11,** e1001527
19. Lonard, D. M., Nawaz, Z., Smith, C. L., and O'Malley, B. W. (2000) The 26S proteasome is required for estrogen receptor-α and coactivator turnover and for efficient estrogen receptor-α transactivation. *Mol. Cell* **5,** 939–948
20. Morin, S., Charron, F., Robitaille, L., and Nemer, M. (2000) GATA-dependent recruitment of MEF2 proteins to target promoters. *EMBO J.* **19,** 2046–2055
21. Kondo, K., Klco, J., Nakamura, E., Lechpammer, M., and Kaelin, W. G., Jr. (2002) Inhibition of HIF is necessary for tumor suppression by the von Hippel–Lindau protein. *Cancer Cell* **1,** 237–246
22. Li, Y. H., Reddy, A. K., Taffet, G. E., Michael, L. H., Entman, M. L., and Hartley, C. J. (2003) Doppler evaluation of peripheral vascular adaptations to transverse aortic banding in mice. *Ultrasound Med. Biol.* **29,** 1281-1289
23. Cieslik, K. A., Taffet, G. E., Carlson, S., Hermosillo, J., Trial, J., and Entman, M. L. (2011) Immune-inflammatory dysregulation modulates the incidence of progressive fibrosis and diastolic stiffness in the aging heart. *J. Mol. Cell Cardiol* **50,** 248–256
24. Taffet, G. E., Hartley, C. J., Wen, X., Pham, T., Michael, L. H., and Entman, M. L. (1996) Noninvasive indexes of cardiac systolic and diastolic function in hyperthyroid and senescent mouse. *Am. J. Physiol.* **270,** H2204–H2209
25. Baskin, K. K., and Taegtmeyer, H. (2011) AMP-activated protein kinase regulates E3 ligases in rodent heart. *Circ. Res.* **109,** 1153–1161